■ EXPERIMENTAL SCIENCE ■

Real-Time Ultrasound Elastographic Imaging of Ocular and Periocular Tissues: A Feasibility Study

Efstathios T. Detorakis, MD, PhD; Eleni E. Drakonaki, MD; Miltiadis K. Tsilimbaris, MD, PhD; Ioannis G. Pallikaris, MD, PhD; Spiridon Giarmenitis, MD, PhD

■ **BACKGROUND AND OBJECTIVE:** This study examines the value of ultrasound elastography for the examination of ocular and periocular structures.

■ **SUBJECTS AND METHODS:** Five patients, aged 22 to 75 years, who each had one blind eye were included. Patients underwent ultrasound elastography of their blind eye and periocular tissues using a 7-13 MHz probe. Strain grayscale and color-coded elastographic maps were recorded. In the former, a quantitative assessment of signal intensity (corresponding to elastic properties) for specific anatomical structures was performed.

■ **RESULTS:** Anterior vitreous displayed intermediate elasticity, whereas posterior vitreous displayed low elasticity. Medial and lateral rectus muscle elasticity was higher in primary position than in adduction or abduction.

■ **CONCLUSION:** The pattern of elastic imaging in the vitreous cavity could be attributed to posterior vitreous detachment, whereas that of medial and lateral rectus muscles may be related to the level of muscle fiber strain.

[Ophthalmic Surg Lasers Imaging 2010;41:135-141.]

INTRODUCTION

The determination of the elasticity of living tissues has been used as an important indicator of disease because the mechanical properties of diseased tissue are typically different from those of the normal tissue surrounding them.[1] Elastography is a method of imaging and measuring the elastic properties of tissues based on static compression and cross-correlation methods.[2] The main elastographic techniques include magnetic resonance elastography and ultrasound elastography.[3] In the former method, constrained modulus reconstruction techniques have been employed, assuming that the geometry of normal and suspicious tissues is available from magnetic resonance imaging segmentation.[3] In the latter method, the footprint of the ultrasound probe is used to compress the tissues axially and tissue axial displacements are estimated with cross-correlation analysis applied to pre-decompression and post-decompression echoes.[3]

By employing ultrasound elastography, a variety of normal and diseased living human tissues and organs have been evaluated, including lymph nodes,[4] prostate,[5] articular cartilage,[6] pancreas,[7] kidney,[8] skin,[9] and breast.[10] Through the development of ultra-fast algorithms tailored to suitable hardware, ultrasound elastography can currently be performed in a typical clinical ultrasound

From the Departments of Ophthalmology (ETD, MKT, IGP) and Medical Imaging (EED, SG), University Hospital of Heraklion, Crete, Greece.

Accepted for publication March 30, 2009.
The authors have no financial or proprietary interest in the materials presented herein.
Address correspondence to Efstathios T. Detorakis, MD, Department of Ophthalmology, University Hospital of Heraklion, Crete, Greece.
doi: 10.3928/15428877-20091230-24

TABLE 1
Demographic and Clinical Characteristics of Patients Studied

Patient	Gender	Age (Y)	Eye Studied	Cause of Visual Loss
1	Male	75	Left	Optic neuropathy
2	Male	62	Right	Absolute glaucoma
3	Female	28	Left	Absolute glaucoma
4	Male	22	Left	Optic neuropathy
5	Female	58	Right	Retinal detachment

setting at quasi real-time (approximately at a frame rate of 8 frames/sec) and with the use of a handheld transducer (as opposed to the previously used frame-suspended set-up), during and simultaneously with an ultrasound examination.[1] In this study, we present findings from ultrasound elastography in living human ocular and periocular tissues. It is a preliminary feasibility study in blind eyes, which could help in determining the potential role of ultrasound elastography in the evaluation of normal and diseased ocular and periocular tissues.

SUBJECTS AND METHODS

Patients were recruited from the Department of Ophthalmology of the University Hospital of Heraklion, Crete, Greece. Elastography imaging was performed at the Department of Medical Imaging of the University Hospital of Heraklion, Crete, Greece. Five adult patients, three men and two women, who had suffered permanent and complete (no light perception) vision loss in one eye were studied. The examination of blind eyes was based on safety issues because the use of acoustic radiation force as the stressing agent may require intensities exceeding those allowed by the U.S. Food and Drug Administration.[11] Participants gave written informed consent to a protocol approved by the Institutional Review Board in conformity with the tenets of the Declaration of Helsinki.

Mean subject age (± standard deviation) was 52 ± 7 years, with a range of 22 to 75 years. Demographic and clinical characteristics of subjects studied, including age, gender, and cause of unilateral blindness, are presented in Table 1. A medical and ophthalmic history was recorded from each patient. A comprehensive ophthalmic examination was also performed, including applanation tonometry, corneal pachymetry, and axial length measurement of the examined eye.

Each subject underwent combined ultrasound B-mode and elastography imaging of the blind eye and ipsilateral orbit. All elastographic studies were performed by the same experienced examiner (EED). A commercially available ultrasound system (Siemens Antares, Premium Edition; Siemens Medical Solutions, Erlangen, Germany), equipped with specific software to perform elastography (eSie-touch elasticity; Siemens Medical Solutions), was used. The ultrasound examination of all volunteers included B-mode scanning (using a 7-13 MHz probe) and real-time freehand elastography.

Subjects were examined in the supine position. An adequate amount of coupling gel was applied over the gently closed eyelids. Real-time freehand elastography was performed by applying subtle manual compression with the transducer over the region of interest (ROI). The ROI was set to include the eyeball and adjacent orbital structures. Measurements were recorded in a transverse section through the equator of the eyeball. The B-mode and elastographic images (color and grayscale) were displayed side-by-side on a split-screen display. In the case of grayscale elastographic images, the lower luminosity signal (darker) represented areas of lower elasticity, whereas the higher luminosity signal (brighter) represented areas of higher elasticity. In the case of color-coded (pseudo-chromatic) real-time images (superimposed on the B-mode image), the color code indicated the relative stiffness of the tissues within the ROI and ranged from red (most stiff) to blue (least stiff). Green and yellow colors indicated intermediate stiffnesses. Color-coded images were constructed automatically with the same settings throughout all studies. To ensure reproducibility, three compression-relaxation cycles were applied to the orbit and the images were stored as cine-loops in the memory of the ultrasound system. To ensure correct application of the technique, only the images where the elastogram consistently overlapped with the B-mode image were used for evaluation.

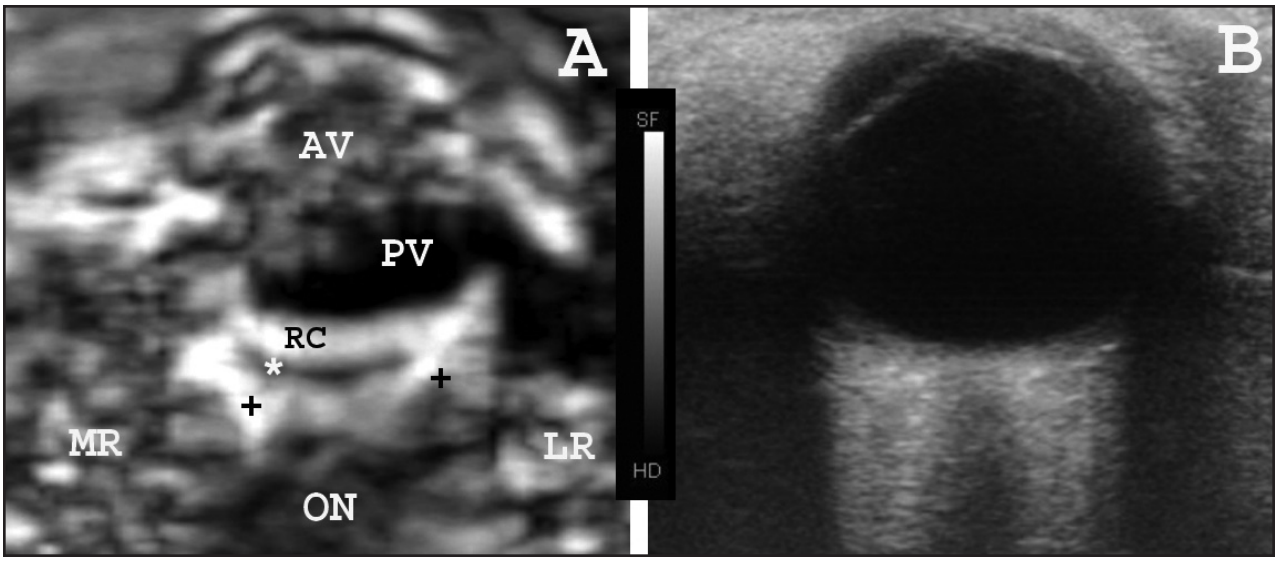

Figure 1. Grayscale ultrasound transverse elastographic image of (A) an eye and orbit and (B) corresponding B-scan image. The retina and choroid (RC) are presented with higher luminosity (more elastic) than the sclera (*). The intraconal fat pads (+) lateral and medial to the optic nerve are also shown with a higher luminosity (more elastic). The medial and lateral rectus muscle (MR and LR, respectively) and the optic nerve (ON) are shown with intermediate luminosity. The anterior vitreous cavity (AV) is shown with intermediate luminosity (intermediate elasticity) compared with the posterior vitreous cavity (lower luminosity and, therefore, lower elasticity). The gray scale from white (more elastic) to black (less elastic) is shown between A and B.

Subjects were imaged with the eyes in primary position, adduction, and abduction. Transverse sections (through the equator of the globe) were examined. The optic nerve dark zone was identified in all cases and used as a landmark for the imaging of the ocular and orbital structures, including the anterior and posterior vitreous cavity, medial and lateral intraconal orbital fat pads, and medial and lateral rectus muscles. In one case (case 5 in Table 1, suffering from chronic retinal detachment), the elastic properties of detached retina and subretinal fluid were also examined. Digital grayscale elastographic images were quantified and analyzed using eFilm workstation (eFilm Medical Inc., Toronto, Ontario, Canada) and the image processing toolbox of the EvoRad RIS/PACS system (EvoRad, Athens, Greece).

The cross-sectional area of imaged structures, including the anterior and posterior vitreous cavity (anterior and posterior to the globe equator), posterior sclera (between the medial and lateral rectus insertions), and optic nerve and intraconal fat pads (between the optic nerve and medial or lateral rectus muscle) were delineated at transverse sections nearest to the equator of the eyeball. The mean luminosity signal of the delineated structures was measured (histogram, luminosity channel) using Adobe Photoshop, version 7.0 (Adobe, San Jose, CA). Likewise, the medial and lateral rectus muscles were delineated in primary gaze, adduction, and abduction. The mean luminosity signal of delineated muscles in adduction and abduction was also recorded and respective values between different gaze positions were compared (paired-samples *t* test). Statistical analyses were performed using SPSS 8.0 software (SPSS, Inc., Chicago, IL).

RESULTS

Elastographic imaging of ocular and periocular structures resulted in reproducible findings in all subjects examined in this study. In grayscale images, the intraconal orbital fat pads appeared with a higher luminosity signal (more elastic) than the optic nerve and medial and lateral rectus muscles (Fig. 1B). At the posterior pole of the globe, a rim of lower luminosity signal (less elastic tissue) appeared interlaced between two rims of higher luminosity signal (more elastic tissue), as presented in Figure 1B. These possibly corresponded to the sclera (less elastic rim), retina and choroid (more elastic rim at the inner surface of the globe), and intraconal fat pads (more elastic rim at the inner surface of the globe laterally and medially to the optic nerve). The iridolenticular area and anterior vitreous cavity appeared of intermediate luminosity (intermediate elasticity) in all subjects, whereas the posterior vitreous cavity appeared of lower

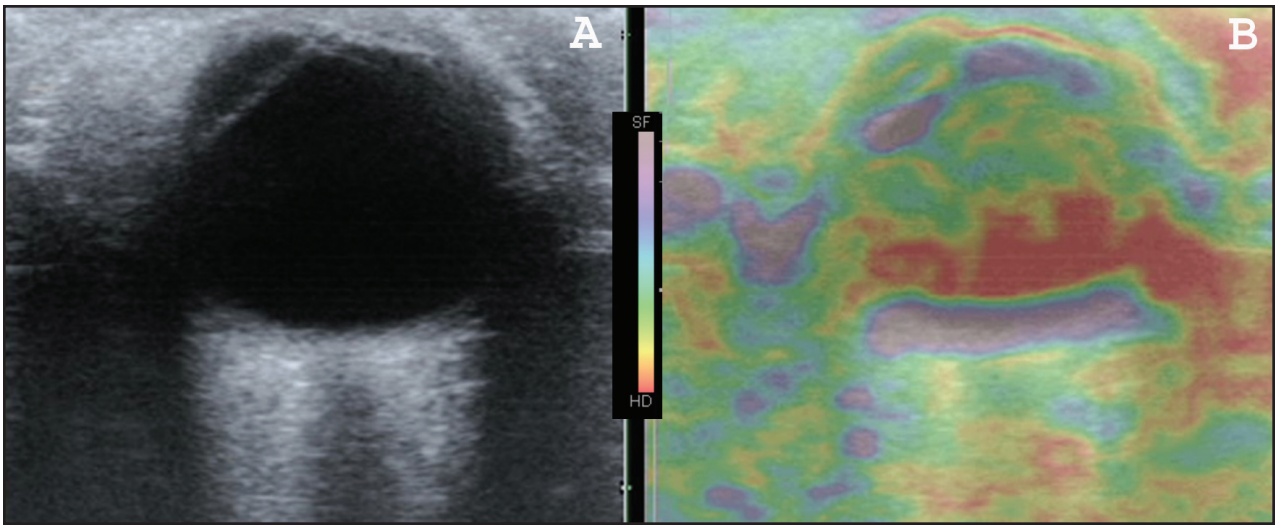

Figure 2. Color-coded ultrasound transverse elastographic image of the same eye presented in Figure 1 (B) and corresponding B-scan image (A). The color scale from blue (more elastic) to red (less elastic) is shown between A and B.

TABLE 2

Mean Area Delineated and Mean Luminosity Values (Mean ± SD) of Optic Nerve, Medial and Lateral Intraconal Fat Pads, Anterior and Posterior Vitreous Cavity, and Posterior Sclera

Delineated Structure	Area (mm^2, Mean ± SD)	Luminosity (Mean ± SD)
Optic nerve	92.1 ± 16.9	69.4 ± 22.8
Medial and lateral intraconal fat pads	141.2 ± 24.2	100.6 ± 32.4
Anterior vitreous cavity	130.1 ± 19.1	96.3 ± 27.5
Posterior vitreous cavity	113.0 ± 40.3	25.1 ± 10.6
Posterior sclera	104.2 ± 18.1	34.2 ± 12.9

SD = standard deviation.

luminosity (less elastic). A color-coded image and corresponding B-scan image of an eye and periocular tissues are presented in Figure 2 (same eye as in Fig. 1). Mean luminosity values of optic nerve, intraconal fat pads, lateral and medial rectus muscles (primary gaze position), anterior and posterior vitreous cavity, and posterior sclera are presented in Table 2.

Detached retina in an eye with chronic retinal detachment appeared as a band of high elasticity embedded with the posterior vitreous cavity. In the same eye, subretinal fluid appeared with lower luminosity signal (less elastic), retinal pigment epithelium and choroidal layers appeared with intermediate luminosity (intermediate elasticity), and sclera appeared with low luminosity (lower elasticity). An eye with chronic retinal detachment is presented in Figure 3 (B-scan and grayscale elastographic map) and Figure 4 (B-scan and color-coded elastographic map).

The optical densities of the medial and lateral rectus muscles were significantly decreased in both adduction and abduction compared with the primary gaze position (Table 3). Grayscale ultrasound elastographic images of the lateral rectus muscle in primary position and abduction are presented in Figure 5. Color-coded elastographic images of the medial rectus muscle in primary position and adduction are presented in Figure 6.

DISCUSSION

This study evaluated the feasibility of performing ultrasound elastography in ocular and periocular tissues by employing a commercially available system. Results imply that the technique is feasible and can provide information of the elasticity of ocular and periocular tissues that may have clinical implications in various conditions.

Results from several previous studies employing ultrasound elastography in the in vivo examination of vari-

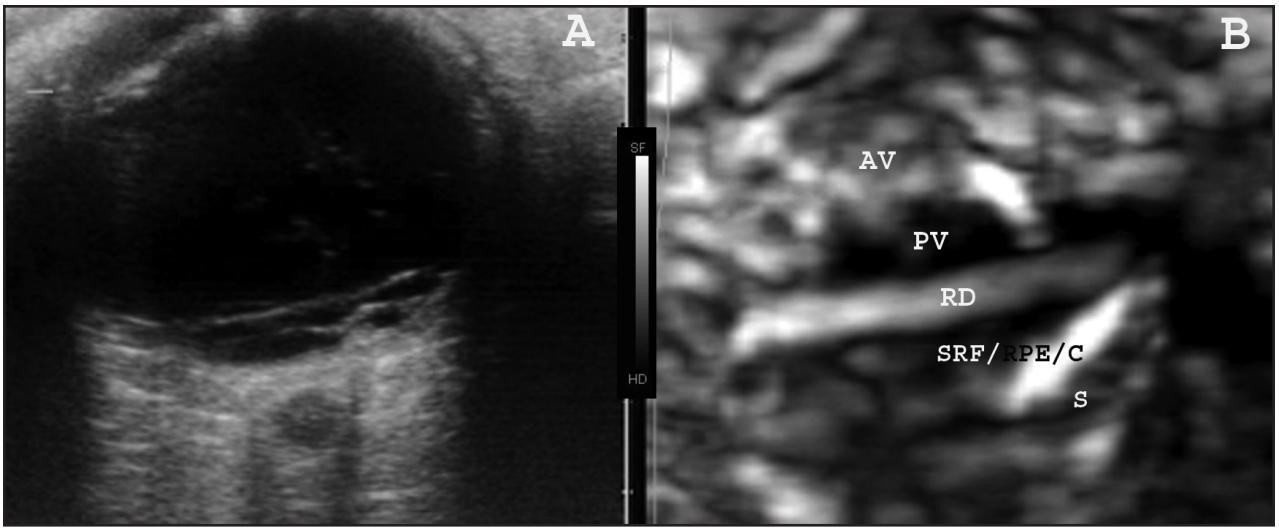

Figure 3. Grayscale ultrasound transverse elastographic image of an eye with chronic retinal detachment (B). The detached retina (RD) appears more elastic (with higher luminosity), compared with the posterior vitreous cavity (PV) and long-standing (viscous) subretinal fluid (SRF). The complex of retinal pigment epithelium (RPE) and choroid (C) also appears with a high luminosity (elastic), whereas the anterior vitreous cavity (AV) appears with intermediate luminosity. On the contrary, the sclera (S) is shown with a low luminosity (inelastic). A corresponding B-scan image is also presented (A), whereas the gray scale from white (more elastic) to black (less elastic) is shown between A and B.

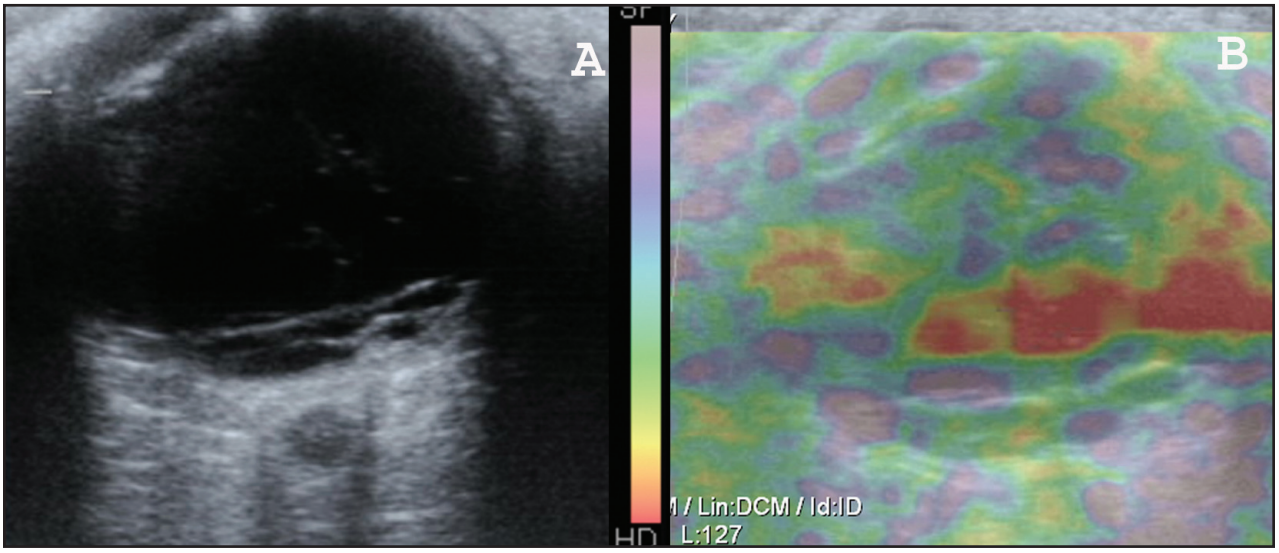

Figure 4. Color-coded ultrasound transverse elastographic image of the same eye presented in Figure 3 (B) and corresponding B-scan image (A). The color scale from blue (more elastic) to red (less elastic) is shown between A and B.

TABLE 3

Mean Luminosity Signal of the Medial and Lateral Rectus Muscles in Primary Position, Adduction, and Abduction, and Statistical Significance of Respective Differences

Muscle	Adduction	*P*[a]	Primary	*P*[a]	Abduction
Medial rectus	21.1 ± 13.4	.11	25.8 ± 12.1	.15	22.3 ± 14.0
Lateral rectus	23.1 ± 17.8	.23	25.7 ± 14.3	.16	22.9 ± 16.7

[a]*Paired samples* t *test.*

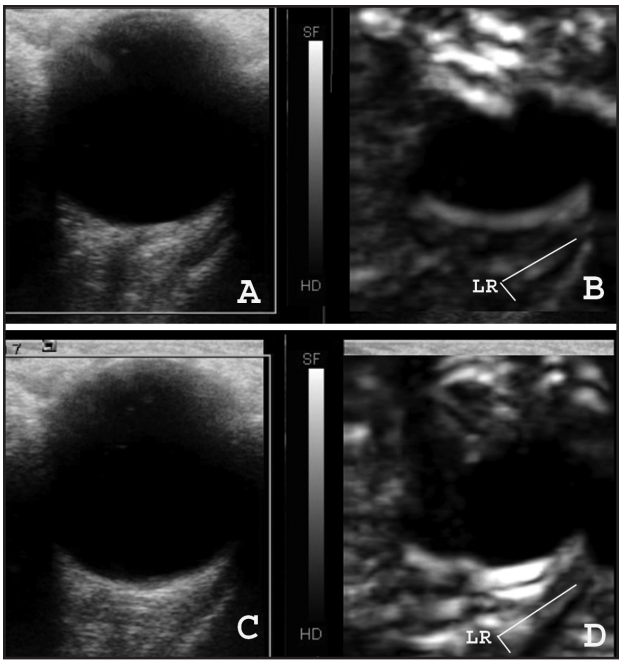

Figure 5. Transverse B-scan images (A and C) and respective grayscale ultrasound elastographic images (B and D) of an eye in primary position (A and B) and abduction (C and D). The lateral rectus muscle (LR) is shown with decreased luminosity (less elastic) in abduction compared with primary position. The gray scale from white (more elastic) to black (less elastic) is also shown.

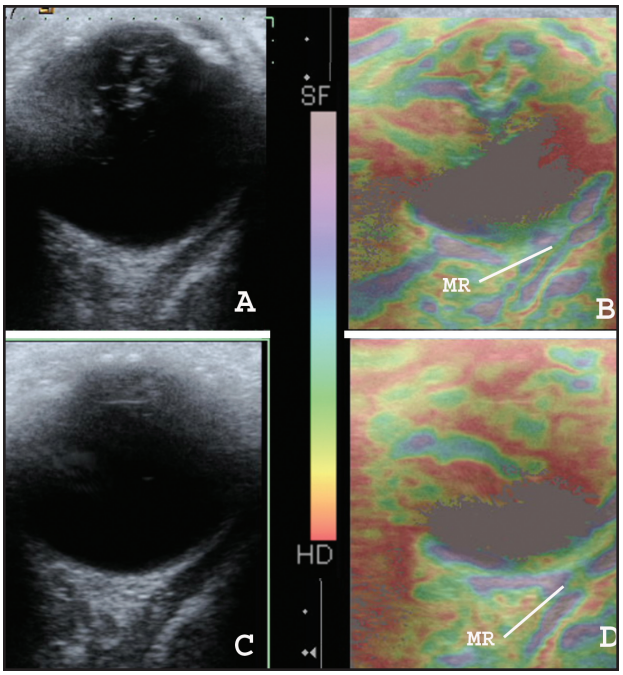

Figure 6. Transverse B-scan images (A and C) and respective color-coded ultrasound elastographic images (B and D) of an eye in primary position (A and B) and adduction (C and D). The central portion of the medial rectus muscle (MR) displays a different color pattern in adduction (red-yellow) than in primary position (blue-green), implying decreased elasticity in the latter condition. The color scale from blue (more elastic) to red (less elastic) is also shown.

ous tissues, other than ocular and periocular structures, imply that the technique can accurately assess the mechanical properties of tissues, differentiate normal from abnormal tissues, and provide indications for the nature of tumors.[4-10] The eye differs from other organs in which elastography has been applied so far because it is not solid and has a heterogeneous internal structure. The calculation of the elastic modulus of a tissue depends on assumptions on its properties (ideally the tissue should be incompressible, isotropic, and solid).[2] The cyst-like internal configuration and heterogeneous architecture of the eye imply that it may deviate from the previously described ideal elastic tissue model and instead display, at least in part, poroelastic properties (in poroelastic models, a solid skeleton incorporates amounts of fluid within its pores).[2] Nevertheless, the fact that images obtained from all subjects were reproducible and compatible with the histologic characteristics of tissues examined imply that ultrasound electrography may be applied for the study of ocular and periocular structures. The technique is not currently approved by the U.S. Food and Drug Administration for routine ophthalmic applications.[11] However, because the stressing pulse is brief (only a few milliseconds in duration), the potential for damage from temperature increase is minimized and probably does not introduce a serious safety issue.[12]

In the case of the eyeball, the vitreous cavity displayed a heterogeneous appearance in both grayscale and color-coded elastographic images. The signal from the anterior vitreous cavity corresponded to intermediate or high elasticity, whereas the signal from the posterior vitreous cavity corresponded to low elasticity. This finding may be explained by the fact that all eyes examined had posterior vitreous detachment (evident in indirect ophthalmoscopy) and thus the posterior vitreous cavity was filled with aqueous fluid. The latter displayed a low elasticity signal due to its incompressible nature. On the contrary, the degenerated vitreous scaffold (partly compressible) was displaced in the anterior vitreous cavity, which thus displayed an intermediate elasticity signal. However, this finding may also be artefactual, resulting from excessive incoherent fluid motion inside the vitreous cavity under external compression, as has previously been described for thyroid cystic lesions with colloid content.[13]

The fact that the medial and lateral rectus muscles

displayed a signal of lower elasticity with the globe in primary gaze position and a signal of higher elasticity in adduction or abduction (although not at a statistically significant level) may reflect the tension status of muscle fibers in these muscles in different gaze directions. The possibility of evaluating the elastic properties of extraocular muscles by ultrasound elastography may be applied in conditions in which muscle rigidity is altered, such as Graves' orbitopathy, in which restrictive fibrotic changes render the affected tissues inelastic.[14] Therefore, if normative data are collected on the elasticity of extraocular muscles, ultrasound elastography could have diagnostic value in the diagnosis of Graves' orbitopathy and possibly in the differential diagnosis between Graves' orbitopathy and orbital myositis, which is a common clinical question.

The quantitative evaluation of the elasticity of the ocular walls may be used in the assessment of the ocular rigidity. The latter is currently indirectly calculated by measuring changes in the intraocular pressure following graded volume displacement and employing normative data from cadaveric eyes (Friedenwald diagram).[15] This method has received criticism because the elastic properties of cadaveric eyes differ from those in living eyes.[15] Although methods of direct measurement of ocular rigidity in living human eyes have been described, they are interventional and include the intraoperative intraocular insertion of manometric probes.[16] The easier noninvasive elastographic examination of ocular rigidity could thus lead to the evaluation of the role of this parameter in various conditions, including glaucoma[17] and age-related macular degeneration,[18] in which rigidity may play a significant pathogenetic role.

Although the current report did not include patients with intraocular or intraorbital tumors, due to its design as a feasibility study it would be reasonable to assume that once the value of ultrasound elastography for ocular and periocular tissues is established its use may be expanded to the evaluation of ocular or periocular neoplastic conditions. The method is already in widespread use for the systematic study of various non-ophthalmic tumors.[4,5,7,8,10] The fact that detached retina was imaged in both grayscale and color-coded elastographic maps implies that the technique can be used for the diagnosis and study of retinal detachment and possibly the differentiation between retinal tissue hemorrhagic or membranous formations in the vitreous cavity.

The small number of patients studied and non-randomized selection may be considered weak points of this study. Furthermore, luminosity signal measurement corresponding to elasticity values was indirectly obtained using Adobe Photoshop 7.0 because the elastography system used did not provide direct luminosity measurements of the structures examined. On the other hand, the fact that all patients were examined by the same examiner using the same technique possibly enhances the validity of results. Future research in this area may set specific normative data of elasticity for ocular and periocular tissues and explore the potential role of ultrasound elastography in the evaluation of various ophthalmic pathological conditions.

REFERENCES

1. Konofagou EE. Quo vadis elasticity imaging? *Ultrasonics.* 2004;42:331-336.
2. Konofagou EE, Harrigan TP, Ophir J, Krouskop TA. Poroelastography: imaging the poroelastic propertied of tissues. *Ultrasound Med Biol.* 2001;27:1387-1397.
3. Luo J, Ying K, Bai J. Elasticity reconstruction for ultrasound elastography using a radial compression: an inverse approach. *Ultrasonics.* 2006;44:195-198.
4. Saftoiu A, Vilmann P, Ciurea T, et al. Dynamic analysis of EUS used for the differentiation of benign and malignant lymph nodes. *Gastrointest Endosc.* 2007;66:291-300.
5. Patil AV, Garson CD, Hossack JA. 3D prostate elastography: algorithm, simulations and experiments. *Phys Med Biol.* 2007;52:3643-3663.
6. Nieminen HJ, Julkunen P, Toyras J, Jurvelin JS. Ultrasound speed in articular cartilage under mechanical compression. *Ultrasound Med Biol.* 2007;3:1755-1766.
7. Janssen J, Schlorer E, Greiner L. EUS elastography of the pancreas: feasibility and pattern description of the normal pancreas, chronic pancreatitis, and focal pancreatic lesions. *Gastrointest Endosc.* 2007;65:971-978.
8. Pareek G, Wilkinson ER, Bharat S, et al. Elastographic measurements of in-vivo radiofrequency ablation lesions of the kidney. *J Endourol.* 2006;20:959-964.
9. Mofid Y, Ossant F, Imberdis C, Josse G, Patat F. In-vivo imaging of skin under stress: potential of high-frequency (20 MHz) static 2-D elastography. *IEEE Trans Ultrason Ferroelectr Freq Control.* 2006;53:925-935.
10. Itoh A, Ueno E, Tohno E, et al. Breast disease: clinical application of US elastography for diagnosis. *Radiology.* 2006;239:341-350.
11. Nightingale KR, Palmeri ML, Nightingale RW, Trahey GE. On the feasibility of remote palpation using acoustic radiation force. *J Acoust Soc Am* 2001;110:625-634.
12. Duck FA. Medical and non-medical protection standards for ultrasound and infrasound. *Prog Biophysics Mol Biol.* 2007;93176-93191.
13. Lyshchik A, Higashi T, Asato R, et al. Thyroid gland tumor diagnosis at US elastography. *Radiology.* 2005;237:202-211.
14. Riemann CD, Foster JA, Kosmorsky GS. Direct orbital manometry in patients with thyroid-associated orbitopathy. *Ophthalmology.* 1999;106:1296-1302.
15. Friedenwald JS. Contribution to the theory and practice of tonometry. *Am J Ophthalmol.* 1937;20:985-1024.
16. Pallikaris IG, Kymionis GD, Ginis HS, Kounis GA, Tsilimbaris MK. Ocular rigidity in living human eyes. *Invest Ophthalmol Vis Sci.* 2005;46:409-414.
17. Agrawal KK, Sharma DP, Bhargava G, Sanadhya DK. Scleral rigidity in glaucoma, before and during topical antiglaucoma drug therapy. *Indian J Ophthalmol.* 1991;39:85-86.
18. Pallikaris IG, Kymionis GD, Ginis HS, Kounis GA, Christodoulakis E, Tsilimbaris MK. Ocular rigidity in patients with age-related macular degeneration. *Am J Ophthalmol.* 2006;141:611-615.